Desalination and Water Treatment
www.deswater.com
51 (2013) 2076–2086
February
Taylor & Francis
Taylor & Francis Group

doi: 10.1080/19443994.2013.734554

Performance analysis of double slope wick-type solar still with varying thermal insulation beneath the wick surface

R. Rajanarthini, K. Shanmugasundaram, B. Janarthanan*

Department of Physics, Karpagam University, Coimbatore 641021, India
Tel. +91 422 2611082; Fax: +91 422 2611043; email: info@karpagam.com

Received 13 July 2011; Accepted 22 August 2012

ABSTRACT

A double slope wick-type solar still has been designed and fabricated with varying thickness of insulation beneath the tilted wick portion and optimum thickness for effective distillation has been presented. Energy balance equations have been written for each element of the still including the climatic parameters such as solar radiation intensity and ambient temperature, and design parameters of the proposed system. Theoretical equations have been developed for heat and mass transfer mechanisms inside the still. The efficiency of the still is found to be 46% for the insulation thickness of 0.06 m beneath the tilted wick portion and sides of the still. It is confirmed that the bottom and sides of the wick-type solar still should be thermally insulated with a minimum thickness of 0.06 m for better production and performance. Moreover, the distilled water obtained has much lesser value of electrical conductivity and minerals as compared to the raw water.

Keywords: Wick-type solar still; Energy balance equation; Heat transfer coefficients; Efficiency

1. Introduction

Two nonseparable items—i.e. energy and water—are the absolute necessity for human beings. In developing countries, safe drinking water is limited to a certain extent to access (WHO 2008). One of the viable methods of producing fresh water from salty or brackish water is solar distillation. Solar distillation is a process to distill brackish/saline water by utilizing solar energy. Solar distillation devices operate under two modes: passive and active. Several researchers have designed many designs of passive solar stills and analyzed the performance. Among the designs, the performance of wick-type solar stills has great potential because of the high productivity and simplicity [1–4].

The effect of climatic, operational, and design parameters on the year round performance of single-sloped and double-sloped solar stills under Indian arid zone conditions has been studied by Garg and Mann [5]. The performance of tilted wick with the external reflector has shown an increase in distillate output about 21% than conventional solar still [6]. Furthermore, Tanaka and Nakatake [7] have theoretically analyzed the wick-type solar still with a vertical flat plate reflector and found that distillate yield increased by 41%.

Janarthanan et al. [8] have carried out the regenerative effect for floating cum tilted wick solar still and found the increase of production during peak sunny hours. The introduction of charcoal along with the wick surface has increased the yield by 15% [9]. Velmurugan et al. [10] have connected solar pond, stepped solar still and single basin solar still/wick-type solar still in series, and found the increase of productivity for the modification made. Kalidasa Murugavel et al. [11] has concluded that the rubber is the best material to

*Corresponding author.

improve the absorption, storage, and evaporation effect in the basin-type solar still. Zhani et al. [12] have designed humidification–dehumidification unit and a model has been developed to study the steady state behavior of each component of the still. A transient mathematical model has been developed for s single basin solar still with and without external reflector by El-Sebaii and Al-Dossari [13]. It has been concluded that the annual average production of distilled water is found to be 52.75%, which is higher than that of the still without reflector. Hikmet and Assefi [14] have compared the performance of direct and indirect distillation system briefly. Phadatare and Verma [15] have designed two plastic solar stills with acrylic sheet (3 mm) and glass cover (3 mm) as condensing surface to predict the best condensing surface. It has been found that the still with glass cover has provided 30–35% more output than the still with acrylic sheet. Moreover, Arjunan et al. [16] have used sponge liners on the inner wall of the still and found that the temperature difference between the evaporating and condensing surface increases that leads to the enhancement of productivity of distilled water output. Abdul-Wahab et al. [17] have tested an inverted absorber solar still and obtained 3.5 l/m^2 during 7 am to 7 pm. It has been suggested that thermal insulation layer should be provided under the basin to hold the thermal storage during daytime. Furthermore, Khalifa and Ibrahim [18] have investigated the effect of inner and outer reflectors on the output of simple basin still in summer, autumn, and winter. It has been inferred that the productivity of the still is more in autumn and winter with internal and external reflector except for summer.

Khalifa and Hamood [19] have undergone performance correlations of a basin-type solar still based on research data reported in literature. These correlations have found the effect of brine depth, cover tilt angle, and dye on productivity. Mass transfer inside the simple and hybrid solar still has been found using Lewis, Dunkle and Kumar and Tiwari correlations by Hidouri et al. [20] and concluded that the Lewis correlation has found good agreement with the experimental observations than Dunkle and Kumar and Tiwari correlation.

Arshad et al. [21] have designed and tested a honeycomb double exposure solar still and inferred that the productivity is 25% higher than the ordinary double exposure solar still. Balan et al. [22] have made a detailed review on passive solar distillation systems and reported that the wick-type solar still is better than the basin-type solar stills. Ayber and Assefi [23] have reported the best water depth and glass cover inclination of a simple solar still to provide higher distillate yield in Cyprus. Dwivedi and Tiwari [24] have developed a thermal model of a double slope passive solar still on the basis of energy balance of east and west condensing covers, water mass and basin liner to evaluate the CO_2 emission, mitigation, and carbon credit earned for different water depth and life of the system on the basis of energy and exergy.

Followed by the researchers, Tanaka and Nakatake [25] have made an attempt to compare the performance of wick-type solar still with inclined flat plate external reflector and a vertical reflector. It has been found that the productivity increased by about 15% or 27% greater for inclined flat plate external reflector, provided that the reflector length is half of or same as the still length. Tanaka [6] has proposed a geometric model to calculate the radiation reflected from an external reflector which is inclined backwards. It has been concluded that the reflector has played a vital role in winter season than in summer on the performance of the still.

In the current work, an attempt has been made to design and fabricate a double-sloped single wick solar still with increased thickness of thermal insulation beneath the tilted wick surface and sidewalls. Experiments have been done in the month of February and March 2010 at Karpagam University, Coimbatore, India. It has been observed that the evaporation rate increased due to the presence of thermal insulation in the sidewalls and beneath the evaporating surface, which decreases the side and bottom heat losses from the heart of the still i.e. the tilted wick portion.

2. Design of double slope single wick solar still

The schematic sectional view and photographs of the proposed still have been shown in the Figs. 1 and 2. In the proposed still, the blackened jute wick is spread along with 30° double slope tilted portion and the remaining part of the wick is immersed in the water reservoir. The thermo coal insulation of thickness 6 cm is introduced to the sidewalls and bottom side of the tilted portion to minimize the heat losses from the evaporating wick surfaces. The water level in the reservoir is maintained so as not to overflow into the tilted portion and always to be 0.5 cm below the tilted portion. Due to the raised water level in the reservoir, the tilted wick surfaces were always wet. The excess hot water from the tilted surfaces was fed to the reservoir during late and early working hours of the still.

3. Theoretical analysis

Fraction of solar flux absorbed by the north-facing glass cover is:

$$\alpha_{g1}^{1} = (1 - R_{g1})\ \alpha_{g1} \tag{1}$$

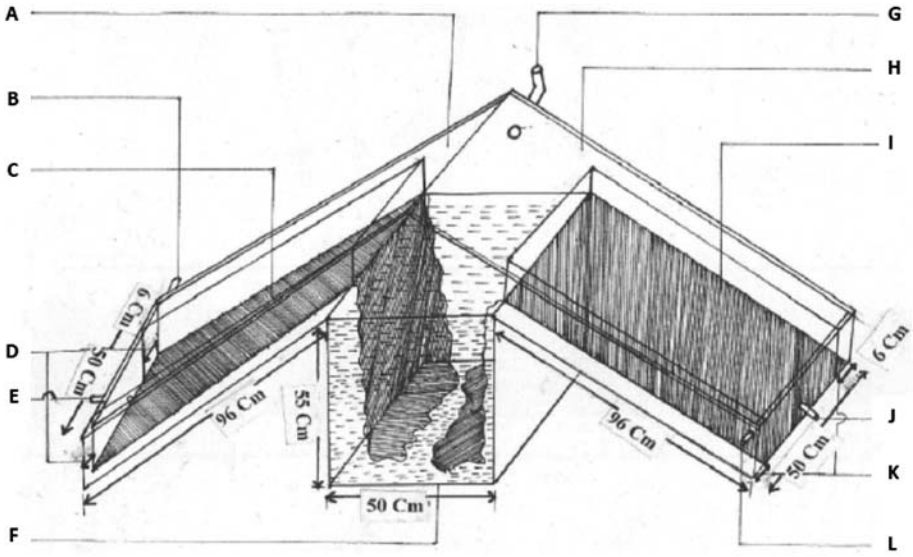

A – North facing cover glass
B – Distillate yield outlet
C – North facing wick surface
H – South facing glass cover
D – 6cm insulation for sidewalls
I – South facing wick surface
E– North facing waste hot water outlet
J– South facing waste hot water outlet
F - Water trough
K – 6cm insulation for sidewalls
G – Saline water inlet
L – Distillate yield outlet

Fig. 1. Schematic sectional view of the proposed still.

Fig. 2. Photograph of the proposed still.

Fraction of solar flux absorbed by the south-facing glass cover is:

$$\alpha^1_{g2} = (1 - R_{g2})\ \alpha_{g2} \tag{2}$$

Fraction of solar flux absorbed by the north-facing wick surface is:

$$A^1_{w1} = \alpha_{w1}\ (1 - \alpha_{g1})\ (1 - R_{g1}) \tag{3}$$

Fraction of solar flux absorbed by the south-facing wick surface is:

$$A^1_{w2} = \alpha_{w2}\ (1 - \alpha_{g2})\ (1 - R_{g2}) \tag{4}$$

Fractions of solar flux lost to the ambient by south- and north-facing wick surface are:

$$L_{w1} = (1 - \alpha_{w1})\ (1 - R_{g1})\ (1 - \alpha_{g1})\ \text{[North-facing]} \tag{5}$$

$$L_{w2} = (1 - \alpha_{w2})\ (1 - R_{g2})\ (1 - \alpha_{g2})\ \text{[South-facing]} \tag{6}$$

At thermal equilibrium, the evaporation process is considered as isobaric and hence all the absorbed

radiation is utilized for evaporation and thermal losses. An energy balance for steady state around the wick surfaces can be written as:

Energy input = Energy output

That is, for north-facing wick surface:

$$\alpha_{w1}\ I(t)\ A_{w1} = Q_{ew1} + Q_{losses,w1} \tag{7}$$

For south-facing wick surface:

$$\alpha_{w2}\ I(t)\ A_{w2} = Q_{ew2} + Q_{losses,w2} \tag{8}$$

where

$$Q_{ew1} = M_{w1} \cdot L \tag{9}$$

$$Q_{ew2} = M_{w2} \cdot L \tag{10}$$

$$Q_{losses,w1} = U_{L1}\ (T_{w1} - T_a)\ A_{w1} \tag{11}$$

$$Q_{losses,w2} = U_{L2}\ (T_{w2} - T_a)\ A_{w2} \tag{12}$$

Using Eqs. (9)–(12), Eqs. (7) and (8) can be written as

$$\alpha_{w1}\ I(t)\ A_{w1} - U_{L1}\ (T_{w1} - T_a)\ A_{w1} = M_{w1} \cdot L \tag{13}$$

$$\alpha_{w2}\ I(t)\ A_{w2} - U_{L2}\ (T_{w2} - T_a)\ A_{w2} = M_{w2} \cdot L \tag{14}$$

The heat transfer occurring outside the still from the glass cover, the bottom and side insulation referred to as external heat transfer mode, which consists of radiation and convection. Heat transfer within the still is referred to as the internal heat transfer mode which consists of radiation, convection, and evaporation.

The external heat transfer—that is radiation and convection losses from the glass cover to the outside atmosphere Q_g can be expressed as

$$Q_g = q_{rg} + q_{cg} \tag{15}$$

where

$$Q_{rg} = \varepsilon_{g1}\sigma\ (T_{g1}^4 - T_a^4) + \varepsilon_{g2}\sigma\ (T_{g2}^4 - T_a^4) \tag{16}$$

$$Q_{cg} = h_{cg1}\ (T_{g1} - T_a) + h_{cg2}\ (T_{g2} - T_a) \tag{17}$$

where
$h_{cg1} = 5.7 + 3.8\,V$ (Watmuff et al. [26])
$h_{cg1} = 5.7 + 3.8\,V$ (Watmuff et al. [26])

Heat is also lost from the wick surfaces to the ambient through the insulation on the bottom of the tilted portion by convection and radiation.

The bottom loss coefficient U_b can be written as:

$$U_b = (1/h_w + 1/h_b)^{-1} = [(1/h_w + 1/(K_i/L_i) + 1/(h_{cb} + h_{rb})]^{-1} \tag{18}$$

The side heat loss coefficient U_s can be written as:

$$U_s = U_b A_{ss}/A_s \tag{19}$$

Since $A_{ss} \ll A_s$ and insulation thickness is large, U_s and U_b can be ignored.

The internal heat transfer mode, that is, heat exchange from the north- and south-facing wick surfaces to the glass cover inside the still is governed by radiation, convection, and evaporation. The only difference between internal and external heat transfer mode is that mass transfer occur within the still.

The wick surfaces and glass covers are considered as the infinite parallel planes and the rate of radiative heat transfer from north- and south-facing wick surfaces to the glass cover is given by:

$$q_{rw1} = \varepsilon_{g1}\ \sigma\ (T_{w1}^4 - T_{g1}^4) = h_{rw1}\ (T_{w1} - T_{g1}) \tag{20}$$

$$q_{rw2} = \varepsilon_{g2}\ \sigma\ (T_{w2}^4 - T_{g2}^4) = h_{rw2}\ (T_{w2} - T_{g2}) \tag{21}$$

where

$$h_{rw1} = \varepsilon_{g1}\ \sigma\ [(T_{w1}^2 + T_{g1}^2)\ (T_{w1} + T_{g1} + 546)]$$

$$h_{rw2} = \varepsilon_{g2}\ \sigma\ [(T_{w2}^2 + T_{g2}^2)\ (T_{w2} + T_{g2} + 546)]$$

The free convection across humid area within the still has occurred by the effect of buoyancy due to density variation in the humid fluid. Hence, the rate of convective heat transfer from wick surfaces to the glass covers can be estimated by:

$$q_{cw1} = h_{cw1}\ (T_{w1} - T_{g1})\ \text{(North-Facing)} \tag{22}$$

$$q_{cw2} = h_{cw2}\ (T_{w2} - T_{g1})\ \text{(North-Facing)} \tag{23}$$

where the convective loss coefficients are given as:

$$h_{cw1} = 0.884\ [(T_{w1} - T_{g1}) + (P_{w1} - P_{g1})\ T_{w1}/(268.9 \times 10^3 - T_{w1})]^{(1/3)}\ \text{(Dunkle[27])} \tag{24}$$

$$h_{cw2} = 0.884\ [(T_{w2} - T_{g2}) + (P_{w2} - P_{g2})\ T_{w2}/(268.9 \times 10^3 - T_{w2})]^{(1/3)}\ \text{(Dunkle[27])} \quad (25)$$

where P_{w1}, P_{g1}, P_{w2}, and P_{g2} are the saturation partial pressure of wick and glass temperatures, respectively.

Cooper [28] have derived an equation for mass transfer coefficient, i.e. evaporative heat transfer coefficient from the evaporating surface to glass cover can be estimated as

For north-facing wick surface:

$$h_{ew1} = 0.0162 \times h_{cw1} \times (P_{w1} - P_{g1})/(T_{w1} - T_{g1}) \quad (26)$$

For south-facing wick surface:

$$h_{ew2} = 0.0162 \times h_{cw2} \times (P_{w2} - P_{g2})/(T_{w1} - T_{g2}) \quad (27)$$

The rate of heat transfer per unit area from the wick surfaces to glass covers can be given as:

$$q_{ew1} = h_{ew1}\ (T_{w1} - T_{g1}) \quad (28)$$

$$q_{ew2} = h_{ew2}\ (T_{w2} - T_{g2}) \quad (29)$$

The hourly distillate yield of the still is given by:

$$M = M_{w1} + M_{w2} \quad (30)$$

$$M = [h_{ew1}\ (T_{w1} - T_{g1}) \times 3,600 + h_{ew2}\ (T_{w2} - T_{g2}) \times 3,600]/\mathrm{L} \quad (31)$$

The thermal efficiency within a given time interval can be determined as:

$$\eta_i\ (\%) = [h_{ew1}\ (T_{w1} - T_{g1}) \times 100 + h_{ew2}(T_{w2} - T_{g2})\ \times 100]/I(t) \quad (32)$$

where $I(t)$ is the amount of solar radiation within a given time interval.

4. Results and discussion

The equations in the theoretical analysis have been employed to determine the results. The variation of solar radiation intensity and ambient temperature on the experimental days with varying insulation thickness beneath the tilted wick portion (0.06, 0.07, 0.05, and 0.04 m) in the month of March 2011 at Karpagam University is shown in Fig. 3. It has been observed that the variation of solar radiation intensity and

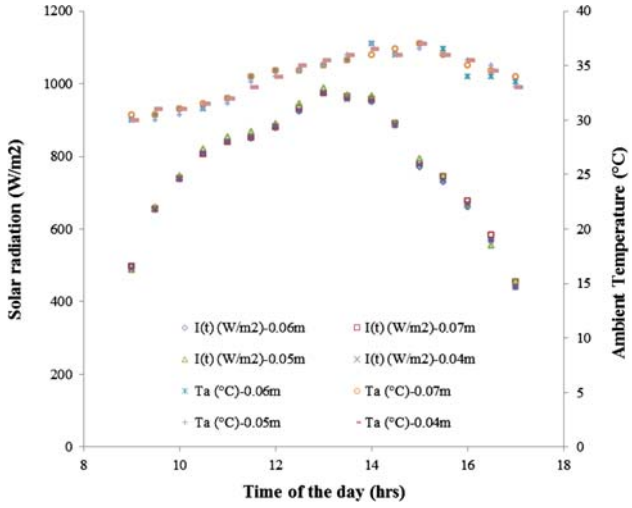

Fig. 3. Variation of solar radiation and ambient temperature.

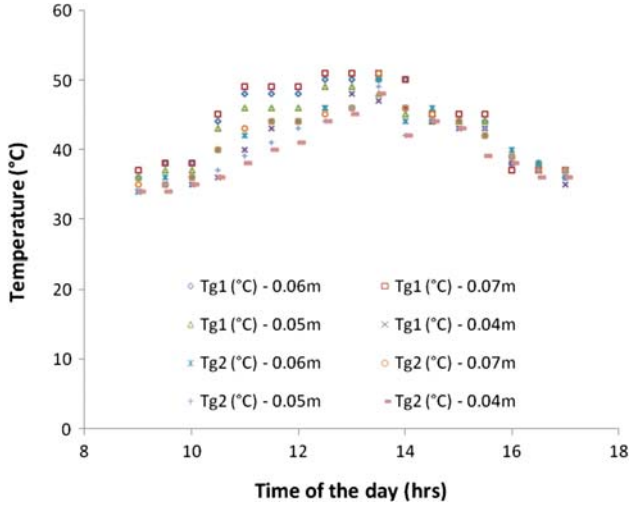

Fig. 4. Variation of glass cover temperature with time.

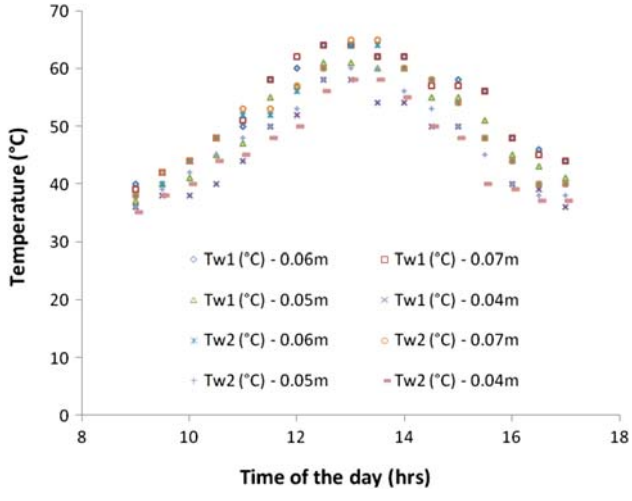

Fig. 5. Variation of wick surface temperature with time.

ambient temperature have same trend for all the experimental days and days are considered as typical days. The average solar radiation and ambient temperature for the experimental days with different insulation thicknesses (0.06, 0.07, 0.05, and 0.04 m) are 771.70, 777.70, 782.64, and 773.17 W/m^2 and 33.88, 34, 33.82, and 33.97˚C.

The temperature of the wick and glass cover surfaces for the corresponding experimental days for varying thickness of insulation beneath the tilted wick portion is shown in Figs. 4 and 5. From the figures, it is observed that, for the insulation thickness of 0.06–0.07 m, the temperature difference between the wick surface and glass cover is more when compared to the thickness of 0.05 m and 0.04 m. The temperature

Table 1
Variation of saturated partial pressures of glass cover temperatures

Time (h)	Pg1 (0.06 m)	Pg1 (0.07 m)	Pg1 (0.05 m)	Pg1 (0.04 m)	Pg2 (0.06 m)	Pg2 (0.07 m)	Pg2 (0.05 m)	Pg2 (0.04 m)
9	4,600	4,850	4,600	4,100	4,100	4,350	4,100	4,100
9.5	5,100	5,100	4,850	4,350	4,600	4,350	4,350	4,100
10	5,100	5,100	4,850	4,350	4,600	4,600	4,350	4,350
10.5	6,600	6,850	6,350	4,600	5,600	5,600	4,850	4,600
11	7,600	7,850	7,100	5,600	6,100	6,350	5,350	5,100
11.5	7,600	7,850	7,100	6,350	6,600	6,600	5,850	5,600
12	7,600	7,850	7,100	6,600	6,600	6,600	6,350	5,850
12.5	8,100	8,350	7,850	7,100	7,100	6,850	6,600	6,600
13	8,100	8,350	7,850	7,600	7,100	7,100	7,100	6,850
13.5	8,100	8,350	7,600	7,350	8,100	8,350	7,850	7,600
14	8,100	8,100	6,850	7,100	6,600	7,100	6,100	6,100
14.5	6,600	6,850	6,600	6,600	7,100	6,850	6,600	6,600
15	6,600	6,850	6,600	6,350	6,600	6,600	6,350	6,350
15.5	6,600	6,850	6,600	6,350	6,100	6,100	6,350	5,350
16	5,100	4,850	5,350	5,100	5,600	5,350	5,350	5,100
16.5	5,100	4,850	5,100	4,850	5,100	4,850	4,850	4,600
17	4,600	4,850	4,850	4,350	4,600	4,850	4,850	4,600

Table 2
Variation of saturated partial pressures of wick surface temperatures

Time (h)	Pw1 (0.06 m)	Pw1 (0.07 m)	Pw1 (0.05 m)	Pw1 (0.04 m)	Pw2 (0.06 m)	Pw2 (0.07 m)	Pw2 (0.05 m)	Pw2 (0.04 m)
9	5,600	5,350	4,850	4,600	5,100	5,100	4,600	4,350
9.5	6,100	6,100	5,600	5,100	5,600	6,100	5,350	5,100
10	6,600	6,600	5,850	5,100	6,600	6,600	6,100	5,600
10.5	7,600	7,600	6,850	5,600	7,600	7,600	6,850	6,600
11	8,100	8,350	7,350	6,600	8,600	8,850	7,600	6,850
11.5	10,100	10,100	9,350	8,100	8,600	8,850	8,100	7,600
12	10,600	11,100	9,850	8,600	9,600	9,850	8,850	8,100
12.5	11,600	11,600	10,850	10,100	10,600	10,600	10,100	9,600
13	11,600	11,600	10,850	10,100	11,600	11,850	10,600	10,100
13.5	11,100	11,100	10,600	9,100	11,600	11,850	10,600	10,100
14	11,100	11,100	10,600	9,100	10,600	10,600	9,600	9,350
14.5	10,100	9,850	9,350	8,100	10,100	10,100	8,850	8,100
15	10,100	9,850	9,350	8,100	9,100	9,100	8,100	7,600
15.5	9,600	9,600	8,350	7,600	7,600	7,600	6,850	5,600
16	7,600	7,600	6,850	5,600	6,600	6,600	5,600	5,350
16.5	7,100	6,850	6,350	5,350	5,600	5,600	5,100	4,850
17	6,600	6,600	5,850	4,600	5,600	5,600	5,100	4,850

difference between the wick and glass cover surfaces increased due to the large thermal insulation beneath the wick surfaces and sidewalls. The side and bottom losses have diminished to a large extent and hence both the north- and south-facing wick surfaces are effectively active during the working hours of the day. The variation of saturated partial pressures of north- and south-facing wick surface and glass cover temperatures is presented in Tables 1 and 2 and Fig. 6. and 7 shows the variation for the same.

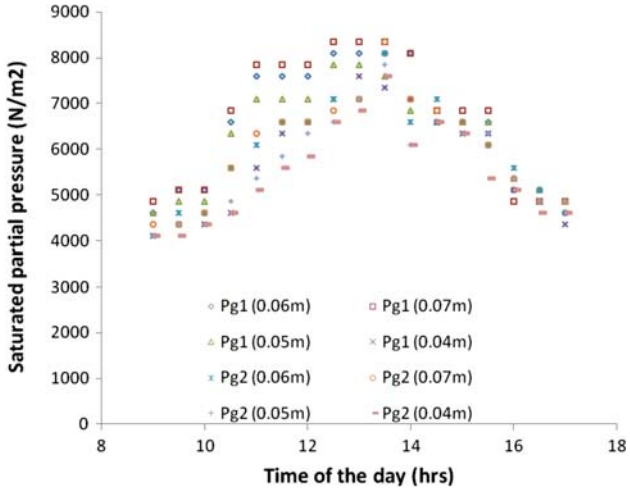

Fig. 6. Variation of saturated partial pressures of glass cover temperature with time.

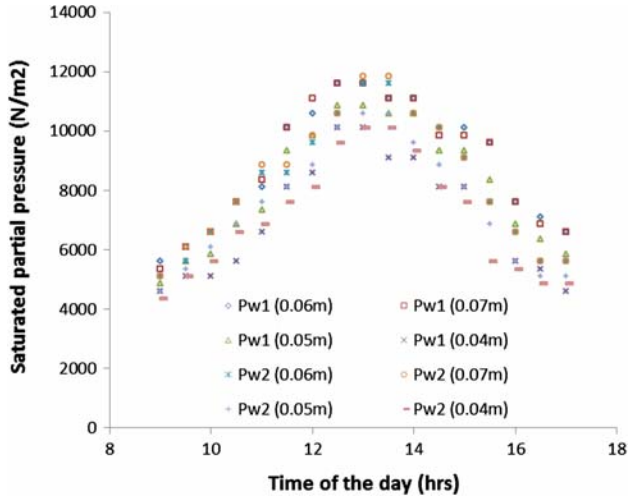

Fig. 7. Variation of saturated partial pressures of wick surface temperature with time.

The convective and evaporative heat transfer coefficients from the north- and south-facing wick surfaces to the glass cover for varying insulation thickness have been found using the equations presented in theoretical analysis and it is shown in the Tables 3 and 4. The plots for the coefficients against time are shown in Figs. 8 and 9 and noticed that the evaporative heat transfer coefficient from the north- and south-facing wick surfaces to the glass cover have shown better characterization curves for the still with 0.06 m thermal insulation thickness beneath the tilted

Table 3
Variation of convective heat transfer coefficient from wick surface to glass cover

Time (h)	hcw1 (0.06 m)	hcw1 (0.07 m)	hcw1 (0.05 m)	hcw1 (0.04 m)	hcw2 (0.06 m)	hcw2 (0.07 m)	hcw2 (0.05 m)	hcw2 (0.04 m)
9	1.530406	1.032189	0.587477	0.739145	1.529439	1.389587	1.21315	0.962575
9.5	1.531376	1.302488	1.093267	1.091844	1.530406	1.845417	1.529922	1.529439
10	1.754101	1.754101	1.148622	1.091844	1.930638	1.930638	1.845417	1.64858
10.5	1.534301	1.394005	1.035386	1.530406	1.933098	1.933098	1.931252	1.930638
11	1.218553	1.35756	1.167877	1.303831	2.08503	2.085698	2.010503	1.847176
11.5	2.08905	1.595346	1.495668	1.298231	1.93557	2.013719	2.011787	1.933098
12	2.221379	1.979209	1.560715	1.199311	2.21852	2.279241	2.085698	2.011787
12.5	2.34153	2.092172	1.499732	1.383929	2.338505	2.392908	2.336998	2.21852
13	2.34153	2.284397	1.499732	0.938724	2.546134	2.593278	2.338505	2.279975
13.5	2.222814	2.253843	1.594431	1.531771	2.34153	2.342289	2.157876	2.08905
14	2.222814	2.125398	1.893955	0.709641	2.444944	2.338505	2.335495	2.277777
14.5	2.336998	2.265036	1.339001	1.386426	2.219947	2.279975	2.013719	1.757458
15	2.336998	2.069031	1.339001	1.298231	2.086367	2.086367	1.850123	1.652776
15.5	2.21852	1.648856	1.145556	0.717899	1.756336	1.756336	1.216613	0.964096
16	2.082367	1.92824	0.827504	1.214684	1.532349	1.650673	0.964096	0.963791
16.5	1.931867	1.553481	1.012933	1.032189	1.214684	1.390466	0.963486	0.963182
17	1.930638	1.523115	0.511471	0.962878	1.530406	1.390466	0.963486	0.963182

Table 4
Variation of evaporative heat transfer coefficient from wick surface to glass cover

Time (h)	hew1 (0.06 m)	hew1 (0.07 m)	hew1 (0.055 cm)	hew1 (0.04 m)	hew2 (0.06 m)	hew2 (0.07 m)	hew2 (0.05 m)	hew2 (0.04 m)
9	6.226075	4.199202	2.390003	3.007025	6.222139	5.653189	4.935399	3.915994
9.5	6.230021	5.298845	4.447684	4.441895	6.226075	7.507619	6.224106	6.222139
10	7.136123	7.136123	4.672883	4.441895	7.854319	7.854319	7.507619	6.706836
10.5	6.24192	5.671161	4.212207	6.226075	7.864326	7.864326	7.856816	7.854319
11	4.957379	5.522892	4.751216	5.304312	8.482423	8.485141	8.179229	7.514775
11.5	8.49878	6.490266	6.084751	5.281527	7.874384	8.192313	8.184453	7.864326
12	9.037125	8.051916	6.349379	4.879099	9.025492	9.272523	8.485141	8.184453
12.5	9.525931	8.51148	6.101283	5.630171	9.513622	9.734947	9.507491	9.025492
13	9.525931	9.293497	6.101283	3.818965	10.35831	10.5501	9.513622	9.275508
13.5	9.042963	9.169198	6.486543	6.231629	9.525931	9.529018	8.778778	8.49878
14	9.042963	8.64665	7.705082	2.886999	9.946643	9.513622	9.501376	9.266565
14.5	9.507491	9.214734	5.447389	5.640329	9.031301	9.275508	8.192313	7.149778
15	9.507491	8.417335	5.447389	5.281527	8.487861	8.487861	7.526761	6.723904
15.5	9.025492	6.707958	4.660407	2.920593	7.145215	7.145215	4.949484	3.922182
16	8.471589	7.844561	3.366493	4.941639	6.233977	6.715349	3.922182	3.920941
16.5	7.859316	6.31995	4.120864	4.199202	4.941639	5.656765	3.919702	3.918465
17	7.854319	6.196411	2.080791	3.917229	6.226075	5.656765	3.919702	3.918465

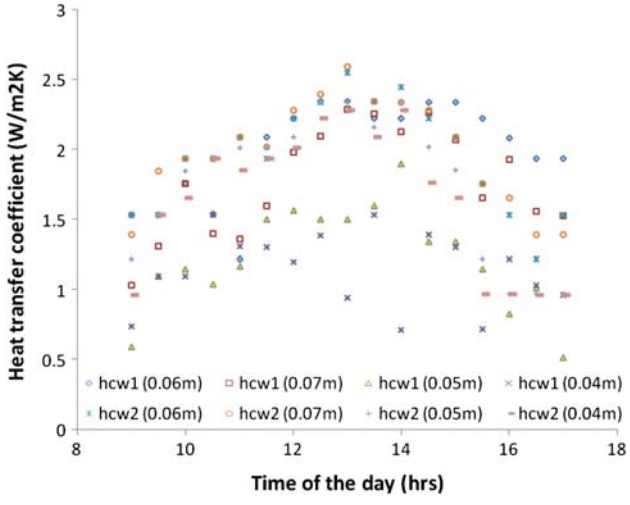

Fig. 8. Variation of convective heat transfer coefficients with time.

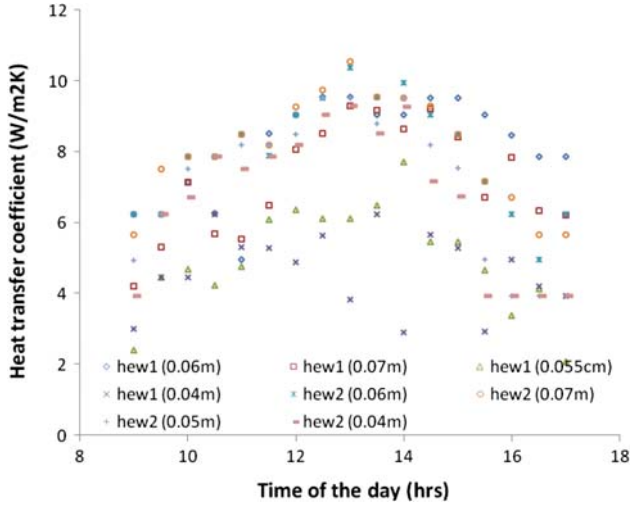

Fig. 9. Variation of evaporative heat transfer coefficients with time.

wick portion and sidewalls. It also has been found that for the thickness of 0.07 m, the coefficients are comparable with the still with thickness 0.06 m. Hence, the optimum thermal insulation beneath the tilted wick portion and sides are found to be 0.06 m.

The distillate yield obtained for north- and south-facing tilted surfaces for varying thickness of thermal insulation beneath the tilted wick portion and sides is shown in Fig. 10. It is found that the rate of evaporation increases due to the increased insulation thickness in sidewalls and beneath the tilted portion. The increased insulation reduces the convection and conduction heat losses from the evaporating surface to the ambient through the insulation. Among the various thickness of insulations, the still with 0.06–0.07 m have shown better distillated yield compared to 0.05 m and 0.04 m thickness. Hence, the optimum thickness of insulation is found to be 0.06 m. The distillate yield is found to be maximum when the solar radiation intensity is maximum. Hence, the distillate

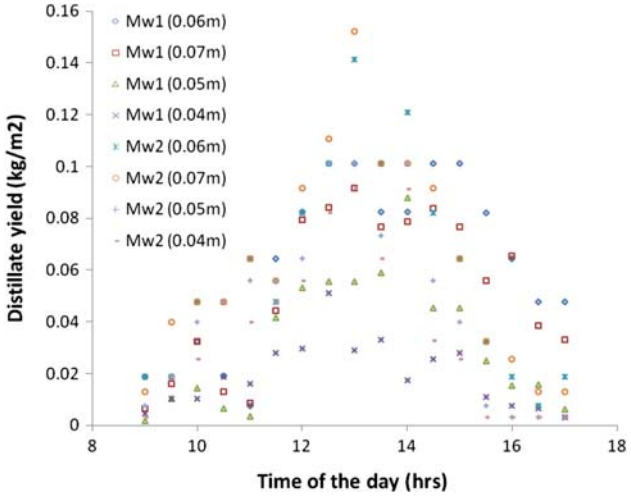

Fig. 10. Variation of distillate yield of north- and south-facing tilted surfaces.

yield resembles the same trend of solar radiation intensity. The instantaneous efficiency of both the portions has been evaluated and is shown in Fig. 11. The instantaneous efficiency is found to be better during 12–2 pm for both north- and south-facing surfaces. A better average instantaneous efficiency of 64.09% has taken place at 1 pm corresponding to the solar radiation intensity of 970 W/m^2 for the insulation thickness of 0.06 m. The average total distillate yield collected during 9 am to 5 pm is 4.0 kg/m^2. The average instantaneous efficiency has been drawn and shown in Fig. 12. The overall efficiency of the still is 46% and the electrical conductivity of the distillate yield has much lesser value and reduced minerals when compared with raw water.

Since the proposed still has shown better performance for the insulation thickness of 0.06 m, the

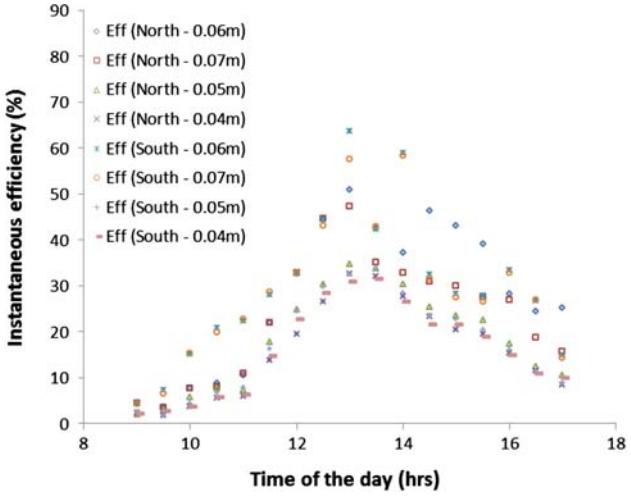

Fig. 11. Variation of instantaneous efficiency for north- and south-facing tilted surfaces.

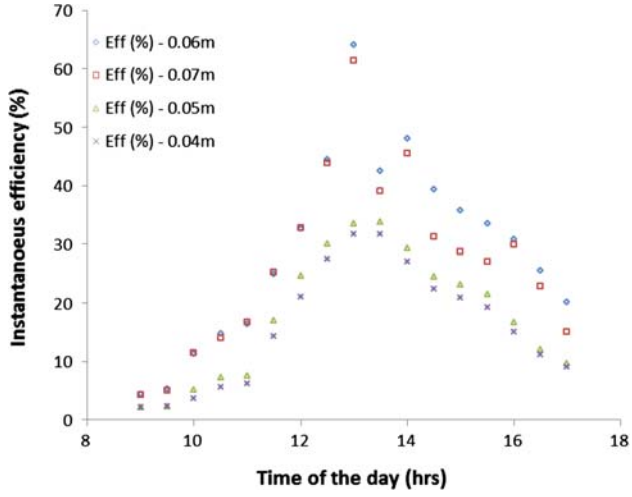

Fig. 12. Variation of average instantaneous of the system.

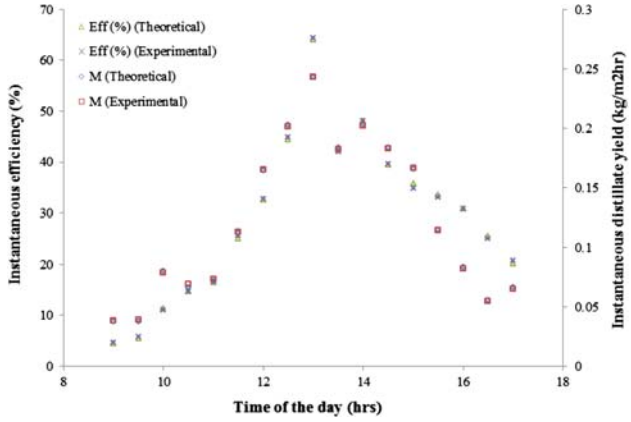

Fig. 13. Variation of theoretical and experimental results of instantaneous distillate yield and efficiency.

theoretical and experimental results of instantaneous distillate yield and efficiency (including the sum of both north- and South-facing wick surfaces) have been plotted and shown in Fig. 13. From the graph, it is clear that the theoretical results are in good agreement with the experimental observations.

The increased insulation thickness in bottom and sides of the proposed still enhanced the evaporative heat transfer leading to large temperature difference between the evaporating and condensing surface as obtained by Arjunan et al. [16] with the sponge liner in the inner side of the still. It also coincides with the results obtained by Janarthanan et al.[2] for single slope floating cum tilted wick-type solar still.

5. Conclusion

Using the heat transfer equations, evaluation of the same has been done and it is seen that there is an

increase in evaporative heat transfer from the wick surfaces to glass cover due to the increased thickness of insulation. The maximum instantaneous efficiency is 64.09% at 1 pm and it is greater than ordinary double slope wick-type solar still with normal insulation and 0.06 m is found to be optimum. In the proposed still the insulation thickness on the sidewalls of the wick surfaces increases the rate of evaporation of water to the glass cover. The thermal performance of the proposed still makes an optimistic hope for the researchers making efforts to produce pure water with overall efficiency of about 46%.

Nomenclature

R_{g1} — reflectance of the north-facing glass cover
R_{g2} — reflectance of the south-facing glass cover
α_{g1} — absorptivity of the north-facing glass cover
α_{g2} — absorptivity of the south-facing glass cover
α_{w1} — absorptivity of the north-facing wick surface
α_{w2} — absorptivity of the south-facing wick surface
$I(t)$ — tilted solar radiation available on the glass cover surface (W/m^2)
Q_{ew1} — total evaporative heat transfer from north-facing wick surface to glass cover (W/m^2)
Q_{ew2} — total evaporative heat transfer from south-facing wick surface to glass cover (W/m^2)
$Q_{losses,\ w1}$ — total heat loss from north-facing wick surface to the ambient (W/m^2)
$Q_{losses,\ w2}$ — total heat loss from south-facing wick surface to the ambient (W/m^2)
U_{L1} — overall heat loss coefficient from north-facing wick surface to ambient (W/m^2 °C)
U_{L2} — overall heat loss coefficient from south-facing wick surface to ambient (W/m^2 °C)
A_{w1} — area of the north-facing wick surface (m^2)
A_{w2} — area of the south-facing wick surface (m^2)
M_{w1} — mass of the distillate yield from north-facing wick surface (kg/m^2 h)
M_{w2} — mass of the distillate yield from south-facing wick surface (kg/m^2 h)
L — latent heat of vaporization of water
Q_g — total external heat transfer from north- and south-facing glass covers to ambient (W/m^2)
q_{rg} — total radiative heat transfer from north- and south-facing glass covers to ambient (W/m^2)
q_{cg} — total convective heat transfer from north- and south-facing glass covers to ambient (W/m^2)
T_{w1} — temperature of the north-facing wick surface (°C)
T_{w2} — temperature of the south-facing wick surface (°C)
T_{g1} — temperature of the north-facing glass cover surface (°C)
T_{g2} — temperature of the south-facing glass cover surface (°C)
T_a — temperature of the ambient (°C)
h_{cg1} — convective heat transfer coefficient from north-facing glass cover to ambient (W/m^2 °C)
h_{cg2} — convective heat transfer coefficient from south-facing glass cover to ambient (W/m^2 °C)
h_{cw1} — convective heat transfer coefficient from north-facing wick surface to glass cover (W/m^2 °C)
h_{cw2} — convective heat transfer coefficient from south-facing wick surface to glass cover (W/m^2 °C)
h_{ew1} — evaporative heat transfer coefficient from north-facing wick surface to glass cover (W/m^2 °C)
h_{ew2} — evaporative heat transfer coefficient from south-facing wick surface to glass cover (W/m^2 °C)
h_{rw1} — radiative heat transfer coefficient from north-facing wick surface to glass cover (W/m^2 °C)
h_{rw2} — radiative heat transfer coefficient from south-facing wick surface to glass cover (W/m^2 °C)
M — total mass of the distillate yield from north- and south-facing wick surfaces (kg/m^2 h)
K_i — thermal conductivity of insulation (W/m^2 °C)
L_i — thickness of insulation (m)
V — wind velocity (m/s)
U_s — total side loss coefficient through the side walls of the still (W/m^2 °C)
U_b — total bottom loss coefficient through the bottom side of the still (W/m^2 °C)
A_s — total area of the still (m^2)
A_{ss} — area of the side walls of the still (m^2)
P_{w1} — saturated vapor pressure at north-facing wick surface temperature (N/m^2)
P_{w2} — saturated vapor pressure at south-facing wick surface temperature (N/m^2)
P_{g1} — saturated vapor pressure at north-facing glass cover temperature (N/m^2)
P_{g2} — saturated vapor pressure at south-facing glass cover temperature (N/m^2)
ε_g — emissivity of glass cover
σ — Stefan-Boltzman constant
$\eta_i(\%)$ — instantaneous efficiency (%)

References

[1] J.T. Mahdi, B.E. Smith, A.O. Sharif, An experimental wick-type solar still system: Design and construction, Desalination 267 (2011) 233–238.

[2] B. Janarthanan, J. Chandrasekaran, S. Kumar, Evaporative heat loss and heat transfer for open and closed cycle systems of a floating tilted wick solar still, Desalination 180 (2005) 291–305.

[3] Hiroshi Tanaka, Tilted wick solar still with flat plate bottom reflector, Desalination 273 (2011) 405–413.

[4] Hiroshi Tanaka, Yasuhito Nakatake, Improvement of the tilted wick solar still by using a flat plate reflector, Desalination 216 (2007) 139–146.

[5] H.P. Garg, H.S. Mann, Effect of climatic, operational and design parameters on the year round performance of single-sloped and double-sloped solar still under Indian arid zone conditions, Sol. Energy 18 (1976) 159–163.

[6] Hiroshi Tanaka, Tilted wick solar still with external flat plate reflector: Optimum inclination of still and reflector, Desalination 249 (2009) 411–415.

[7] H. Tanaka, Y. Nakatake, One step azimuth tracking tilted-wick solar still with a vertical flat plate reflector, Desalination 235 (2009) 1–8.

[8] B. Janarthanan, J. Chandrasekaran, S. Kumar, Performance of floating cum tilted-wick type solar still with the effect of water flowing over the glass cover, Desalination 190 (2006) 51–62.

[9] Mona M. Naim, Mervat A. Abd, El Kawi, Non-conventional solar stills part 1: Non-conventional solar stills with charcoal particles as absorber medium, Desalination 153 (2003) 55–64.

[10] V. Velmurugan, S. Pandiarajan, P. Guruparan, L. Harihara Subramanian, C. David Prabaharan, K. Srithar, Integrated performance of stepped and single basin solar stills with mini solar pond, Desalination 249 (2009) 902–909.

[11] K. Kalidasa Murugavel, Kn.K.S.K. Chockalingam, K. Srithar, An experimental study on single basin double slope simulation solar still with thin layer of water in the basin, Desalination 220 (2008) 687–693.

[12] K. Zhani, H.B. Bacha, T. Damak, Study of a water desalination unit using solar energy, Desalin. Water Treat. 3 (2009) 261–270.

[13] A.A. El-Sebaii, M. Al-Dossari, A mathematical model of single basin solar still with an external reflector, Desalin. Water Treat. 26 (2011) 250–259.

[14] H.Ş. Aybar, H. Assefi, A review and comparison of solar distillation: Direct and indirect type systems, Desalin. Water Treat. 10 (2009) 21–331.

[15] M.K. Phadatare, S.K. Verma, Effect of cover materials on heat and mass transfer coefficients in a plastic solar still, Desalin. Water Treat. 2 (2009) 248–253.

[16] T.V. Arjunan, H.Ş. Aybar, N. Nedunchezhian, Effect of sponge liner on the internal heat transfer coefficients in a simple solar still, Desalin. Water Treat. 29 (2011) 271–284.

[17] Sabah A. Abdul-Wahab, Ali M. Al-Damkhi, Hilal Al-Hinai, Rahul Dev, G.N. Tiwari, Experimental study of an inverted absorber solar still, Desalin. Water Treat. 19 (2010) 249–254.

[18] Abdul Jabbar N. Khalifa, Hussein A. Ibrahim, Experimental study on the effect of internal and external reflectors on the performance of basin type solar stills at various seasons, Desalin. Water Treat. 27 (2011) 313–318.

[19] Abdul Jabbar N. Khalifa, Ahmad M. Hamood, Experimental validation and enhancement of some solar still performance correlations, Desalin. Water Treat. 4 (2009) 311–315.

[20] Khaoula Hidouri, Nejib Hidouri, Romdhane Ben Slama, Slimane Gabsi, Ammar Ben Brahim, Experimental validation of theoretical correlation for calculation of mass transfer in simple and hybrid solar stills, Desalin. Water Treat. 26 (2011) 287–296.

[21] Kutty Arshad, Balasundaram Janarthanan, Sengottain Shanmugan, Performance of double exposure solar still, Desalin. Water Treat. 26 (2011) 260–265.

[22] R. Balan, J. Chandrasekaran, S. Shanmugan, B. Janarthanan, S. Kumar, Review on passive solar distillation, Desalin. Water Treat. 28 (2011) 217–238.

[23] Hikmet Ş. Aybar, Hossein Assefi, Simulation of a solar still to investigate water depth and glass angle, Desalin. Water Treat. 7 (2009) 35–40.

[24] Vijay Kumar Dwivedi, G.N. Tiwari, Thermal modeling and carbon credit earned of a double slope passive solar still, Desalin. Water Treat. 13 (2010) 400–410.

[25] Hiroshi Tanaka, Yasuhito Nakatake, Increase in distillate productivity by inclining the flat plate external reflector of a tilted-wick solar still in winter, Sol. Energy 83 (2009) 785–789.

[26] J.H. Watmuff, W.W.S. Carters, D. Proctor, Solar and wind induced external coefficients for solar collectors, COMPLESW 2 (1977) 56.

[27] R.V. Dunkle, Solar water distillation, International Developments in Heat Transfer, A.S.M.E., Proc. International Heat Transfer, Part V, 1961, pp. 895.

[28] P.I. Cooper, The maximum efficiency of single-effect solar stills, Sol. Energy 15 (1973) 205–214.